EFFECT OF RUST INHIBITOR ON PASSIVE FILM OF REBAR IN CEMENT PASTE UNDER CARBONATION

QUN GUO[1], XIAOZHEN LI[2,3], JUNZHE LIU[1*]
[1]*School of Architecture Engineering, Qingdao Agricultural University, Qingdao, China*
[2] *Faculty of Mechanical Engineering and Mechanics, Ningbo University, Ningbo, China*
[3]*Architectural Engineering Institute, Jinhua Polytechnic, Jinhua, China*

The effect of rust inhibitor on the composition and microstructure of the passive film on the surface of the rebar in carbonated concrete was studied through XPS and other microstructure testing techniques.The mechanism of the rebar passive film formation under the action of rust inhibitor was clarified. The results show that the main components of the passive film are FeOOH, Fe_3O_4,FeO, and Fe_2O_3. The reaction of sodium molybdate (Na_2MoO_4) with Fe^{2+} resulted in the formation of the $FeMoO_4$ protective layer.Benzotriazole (BTA) and Fe combined to form N-Fe bonds, which adhered to the surface of rebar and prevented corrosion. According to the composition and compactness of the passive film, Na_2MoO_4 + BTA has the best corrosion resistance effect.

Keywords: *carbonation; passive film; rust inhibitor; microstructure characteristics*

1. Introduction

In general, due to the highly alkaline concrete pore solution, the surface of the rebar in concrete is in a stable passivation state [1-3]. When the external carbon dioxide diffuses into the concrete, the pH of the pore solution decreases, destroying the passive film and causing corrosion [4-7]. The passive film is the primary barrier to preventing rebar corrosion [8, 9].

In recent years, the research on adding rust inhibitors into concrete to protect rebar has been reported both at home and abroad. Its function is to improve the passivation environment on the rebar surface and protect the morphology of passive film,thereby inhibiting rebar corrosion[10,11].Many factors influence passive film damage, including the surface state of rebar in concrete, alloy composition, iron phase composition, and environmental factors such as the permeability of concrete, chloride concentration, pH, temperature and humidity [12-14]. The thickness, composition and stability of the passive film are affected by polarization potentials, polarization time and ion concentration in the medium.The microstructure characteristics of the passive film are related to the passivation potential and time.The corrosion of rebars is attributed to the changes in the composition and structure of the passive film[15,16]. Therefore, it is critical to understand the mechanism of the rebar passive film's evolution under the action of rust inhibitors to improve the passivation environment of the rebar surface in the concrete.

This paper took the passive film on the rebar surface as the starting point. And the paper focused on the composition and microstructure characteristics of the passive film by adding rust inhibitor and revealed the microstructure evolution law of rebars oxide skin from corrosion to passivation.This provided a theoretical basis for optimizing the composition and structure of passive film, thereby improving the corrosion resistance of rebars in concrete.

2. Experimental program

2.1 Materials and specimen preparation.

Ordinary portland cement with a strength grade of 42.5 was adopted. And HPB235 plain rebar with a diameter of 8mm and thickness of 2mm was used in experiments. Before the rebar was embedded in the cement paste, it was soaked in 10% ammonium citrate solution for five days to remove the surface oxide skin. After taking it out, it was rinsed with water and dried with a towel.Then it was put into the oven at about 100℃ for 10 minutes. After the rebar was polished with sandpaper, it was sealed and wrapped with fresh-keeping film for standby. Anodic rust inhibitors Na_2MoO_4, cathodic rust inhibitors BTA, and the composite units of Na_2MoO_4 and BTA with a concentration of 2.0% were selected in the test. And the compound ratio was 1:1.The size of cement paste specimen was 40 mm × 40 mm × 160 mm, three rebar discs were added inside, and the water-binder ratio was 0.3, as shown in Figure 1.

2.2 Specimen curing and carbonation.

The mold was removed after one day. The specimens were cured for 28 days under standard conditions. Then the specimens were carbonated for 28 days in a carbonation box with 20% CO_2 concentration, 20 ℃ temperature, and 70% relative humidity. The specimens put into the carbonation box were cut horizontally every seven days to observe the color change by spraying

*Autor corespondent/*Corresponding author*,
E-mail: junzheliu@163.com

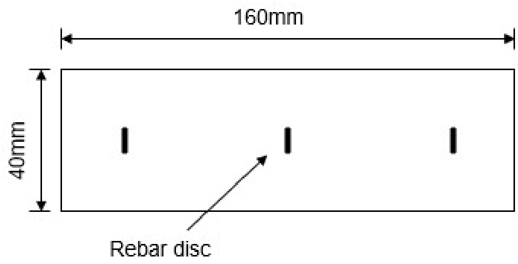

Fig.1 - Schematic diagram of specimen

phenolphthalein. The completely carbonated specimens were placed in natural conditions for 360 days to split. After 360 days, the rebars were taken out to observe the surface corrosion and tested by XPS, XRD, and SEM.

3. Results and discussion

3.1 XPS analysis of the composition of the passive film on rebar surface

Figure 2 is the XPS scanning full spectrum of the passive film on the surface of rebar in cement paste after adding rust inhibitor under the action of carbonation. It can be seen from Figure 2 that the elemental of the passive film is Fe, O, N, C, Ca, Si and Na. N and Na come from rust inhibitor, and the appearance of Si and Ca may be that the elementals in the cement paste participate in the formation of the passive film.Except for Si and Ca, the peaks of O and Fe are very strong. It is preliminarily judged that the main component of passive film is Fe oxide [17-18]. At the same time, the peak of C is also strong, and C comes from the rebar.In Figure 2, it can be seen that the binding energy of Fe 2p in the passive film is 709.93 EV, 711.98 EV, and 709.34 EV. This shows that although the passive film is mainly composed of Fe oxide, the type of rust inhibitor influences the passivation structure of rebar, resulting in different composition of the passive film.

By analyzing the peak fitting diagram of Fe element, the composition of Fe oxide can be known. As shown in Figure 3, the peak curves of Fe 2p of each group are composed of FeOOH, Fe_3O_4, and Fe^{2+}.In addition, there is also Fe^0 in Na_2MoO_4 group. And Fe_2O_3 is present in the Na_2MoO_4 + BTA group.The composition and valence changes of Fe explain the change in the composition of the passive film.The binding energy of Fe element and the relative contents of Fe compounds can be obtained by fitting, as shown in Tables 1-3.It can be seen from Tables 1-3 that the contents of FeOOH in each group exceed 50%, indicating that under the conditions of carbonation, FeOOH is the main component of rebar passive film.Rust inhibitors promote the formation of Fe_3O_4 and Fe^{2+} compounds.FeOOH and Fe_3O_4 play an excellent role in corrosion resistance[19,20].The appearance of Fe° indicates that the rebar in Na_2MoO_4 group does not form a complete passive film.The other two groups do not appear Fe°, indicating that the

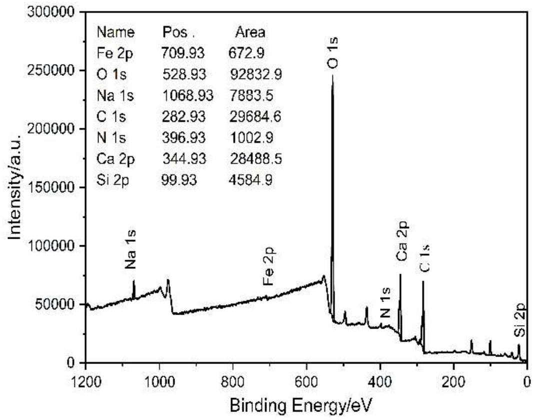

(a)Na_2MoO_4 group

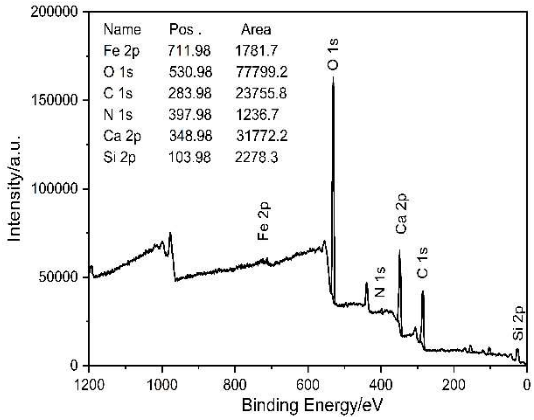

(b)BTA group

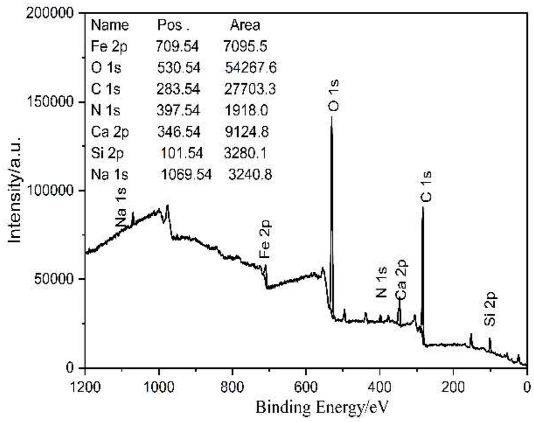

(c)Na_2MoO_4 + BTA group

Fig. 2 - XPS full scan of the passive film on the surface of the rebar in cement paste containing rust inhibitor after carbonation

corrosion resistance effect of Na_2MoO_4 is lower than that of the other two rust inhibitors.Although Na_2MoO_4 can improve the passive film of the rebar, it also causes pitting corrosion within a specific concentration range.However, when Na_2MoO_4 is combined with BTA, the disadvantage of the single type rust inhibitor is improved, and the corrosion resistance effect is improved.

According to the spectrum shown in Figure4(a), the O peaks in each group are composed of FeOOH, Fe_3O_4, and FeO. In addition, there is a Fe_2O_3 peak in Na_2MoO_4 + BTA group.It

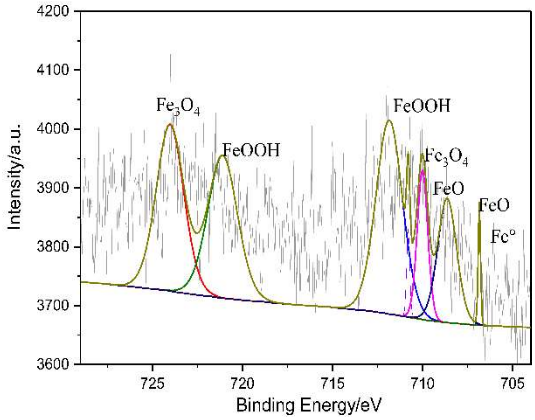

(a)Na_2MoO_4 group

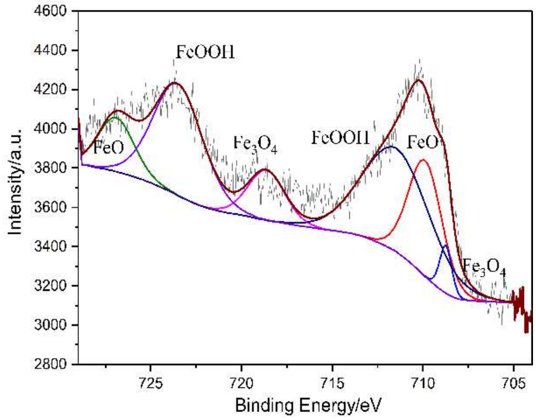

(b)BTA group

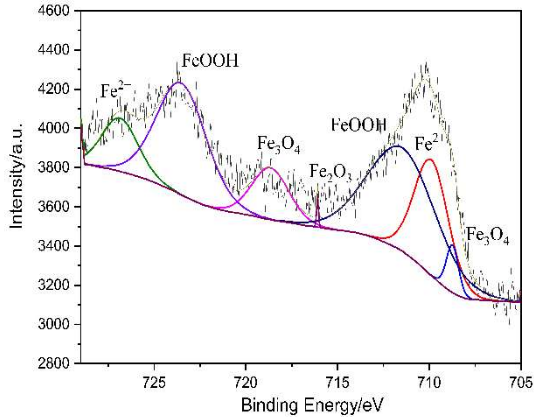

(c)Na_2MoO_4 + BTA group

Fig. 3 - XPS peak fitting diagram of Fe element in passive film on the rebar surface

Table 1

XPS fitting data of Fe element on the surface of rebar in cement paste mixed with Na_2MoO_4

component	Fe 2p energy level	peak binding energy/mV	Half peak width/mV	peak area/(eV)^2	relative content/%
FeOOH	Fe 2p3/2	711.8	1.73	619.4	50.77
	Fe 2p1/2	721.1	1.94	508.7	
Fe_3O_4	Fe 2p3/2	710.9	0.21	33.0	26.41
	Fe 2p1/2	724.0	1.81	553.6	
Fe^{2+}	Fe 2p3/2	710.0	0.69	189.1	21.26
	Fe 2p3/2	708.6	1.24	283.4	
Fe°	Fe 2p3/2	706.8	0.15	34.5	1.56

Table2

XPS fitting data of Fe element on the surface of rebar in cement paste mixed with BTA

component	Fe 2p energy level	peak binding energy/mV	Half peak width/mV	peak area/(eV)^2	relative content/%
FeOOH	Fe 2p3/2	711.5	4.43	2526.8	60.47
	Fe 2p1/2	723.5	3.22	1979.6	
Fe^{2+}	Fe 2p3/2	709.9	2.18	1393.0	27.99
	Fe 2p1/2	726.9	2.33	692.9	
Fe_3O_4	Fe 2p3/2	708.8	0.78	204.4	11.54
	Fe 2p3/2	718.6	2.38	655.6	

Table3

XPS fitting data of Fe element on surface of rebar in cement paste mixed with Na_2MoO_4 + BTA

component	Fe 2p energy level	peak binding energy/mV	Half peak width/mV	peak area/(eV)^2	relative content/%
FeOOH	Fe 2p3/2	711.4	4.42	2526.7	60.47
	Fe 2p1/2	723.5	3.21	1976.9	
FeO	Fe 2p3/2	709.8	2.17	1393.0	28.08
	Fe 2p1/2	726.2	2.32	656.5	
Fe_3O_4	Fe 2p3/2	708.7	0.77	204.4	11.45
	Fe 2p3/2	718.6	2.38	692.9	

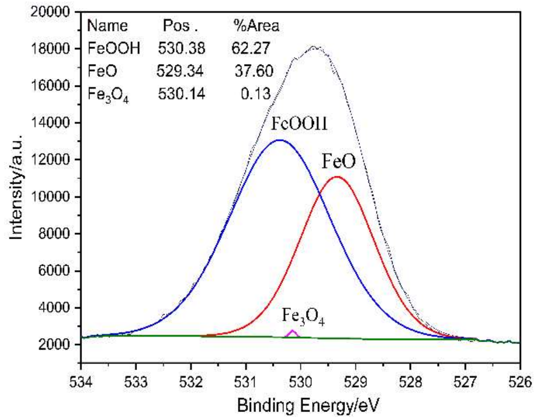

(a)Na_2MoO_4 group

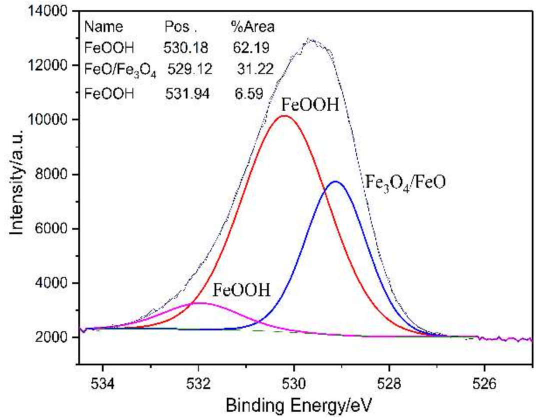

(b)BTA group

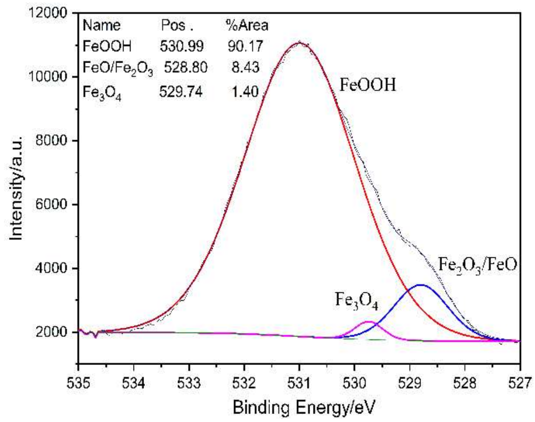

(c)Na_2MoO_4 + BTA group

Fig. 4 - XPS peak fitting diagram of O element in passive film on the rebar surface

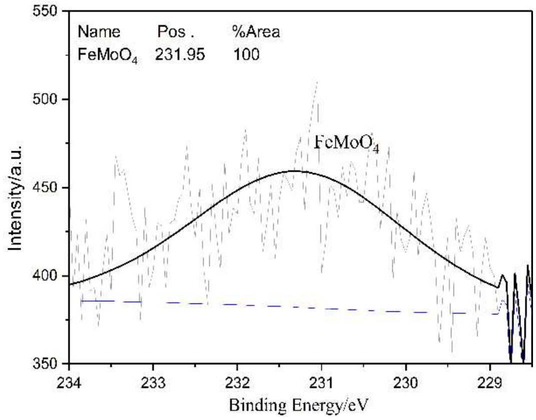

Fig. 5 - XPS spectrum of Mo element on the surface of the rebar in cement paste containing Na_2MoO_4 after carbonation

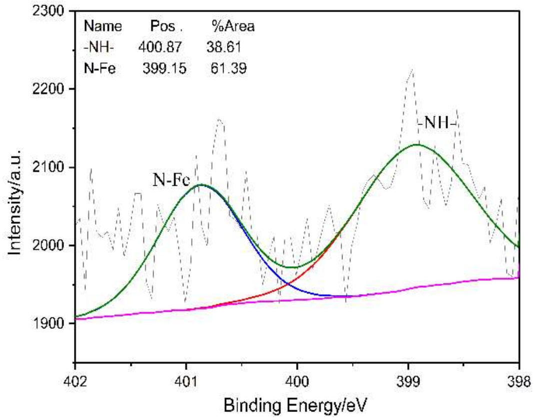

(a)BTA group

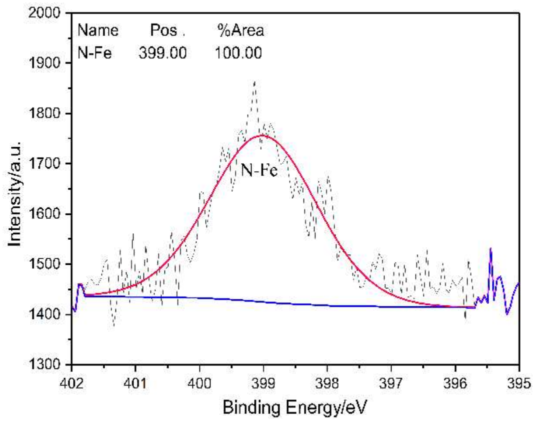

(b)Na_2MoO_4+BTA group

Fig. 6 - XPS peak fitting diagram of N element in passive film on the rebar surface

can be seen from the peak area in Figure 4 that the contents of FeOOH are much greater than that of other components.Based on the above analysis,the results of O 1s analysis of passive film are similar to Fe 2p, and a part of Fe^{2+} is FeO.Figure 5 is the XPS spectrum of Mo element in the passive film. It is found that MoO_4^{2-} reacts with Fe^{2+} to form $FeMoO_4$ protective layer. This reaction indicates that apart of Fe^{2+}in the passive film exists in the form of $FeMoO_4$. Figure 6 shows the XPS peak fitting diagram of N element. It is found that BTA reacts with Fe to form N-Fe bonds, which are adsorbed on the surface of the rebar and play a good role in corrosion resistance. It can be seen in Figure 6 that the relative contents of the N-Fe bond in BTA group are 61.39%, while that in Na_2MoO_4 + BTA group are100%. This indicates that Na_2MoO_4 + BTA has a better corrosion resistance effect compared with BTA

3.2. XRD analysis of the composition of the passive film on rebar surface

The composition of the passive film was analyzed by XRD to judge whether the XPS

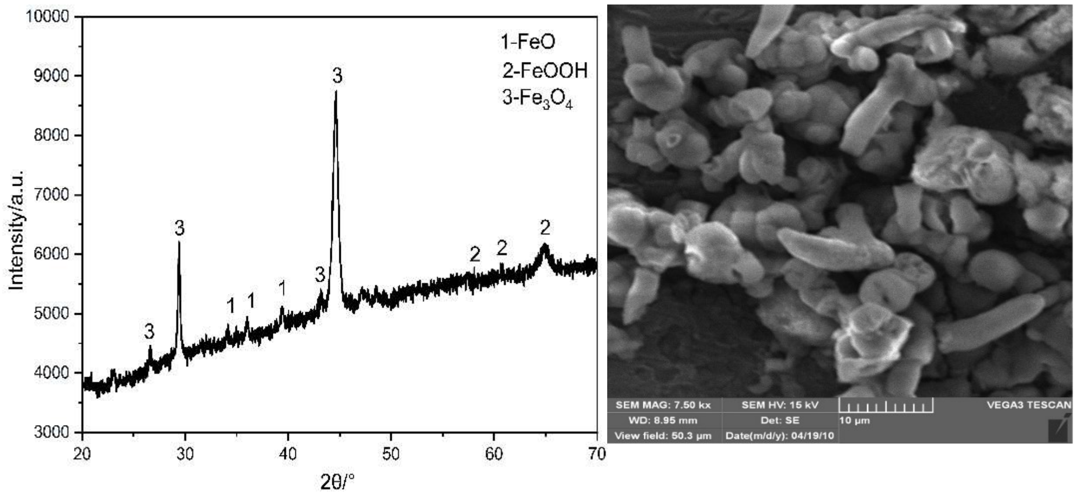

(a)Na_2MoO_4 group

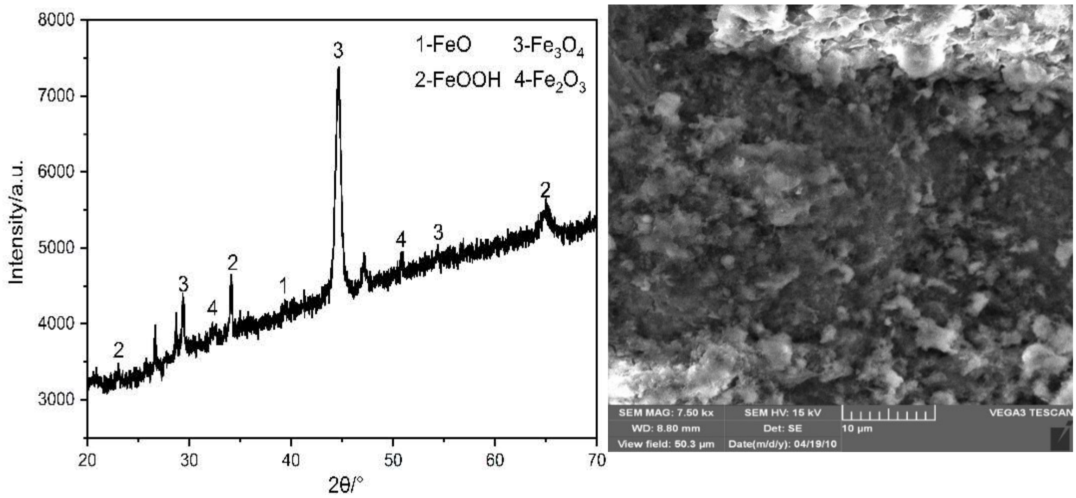

(b)BTA group

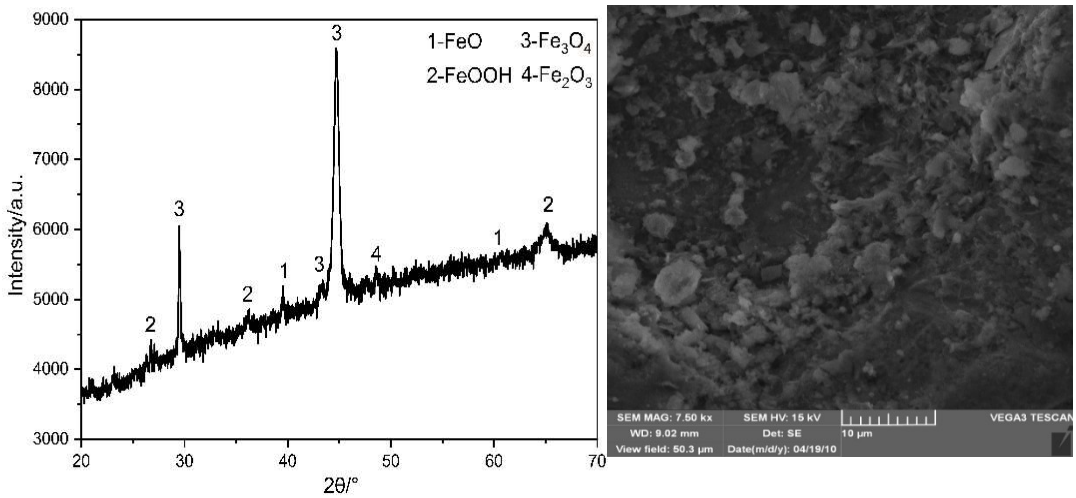

(c)Na_2MoO_4+BTA group

Fig. 7 - X-ray diffraction pattern and micromorphology of the rebar in cement pastecontaining rust inhibitor after carbonation

analysis results were correct. Figure 7 shows the XRD pattern of the passive film on there bar surface. The main diffraction peaks can be seen at 29.1°、44.8° and 64.1°.The main diffraction peaks of each group are for Fe_3O_4 and FeOOH. This shows that the passive film is mainly composed of iron oxide.But there are some differences in small Fe_2O_3, peaks.The small peaks of Na_2MoO_4 group and BTA group are only FeO, while there are Fe_2O_3 peaks in Na_2MoO_4 + BTA group in addition to FeO. The peak intensity of each component in Na_2MoO_4 + BTA group is significantly higher than that in the other two groups.The addition of Na_2MoO_4 and BTA promotes the transformation of FeOOH to stable crystal and the corrosion resistance effect is good.The results of XRD are similar to XPS.It can be seen from SEM that the surface of the rebar in Na_2MoO_4 group is uniformly attached with long strip particles, with loose texture and obvious pore structure.BTA group shows the rebar surface is uneven, butthe compactness is improved compared with the Na_2MoO_4 group.Na_2MoO_4 + BTA group indicates that the rebar surface is attached with granular substances, with fewer pores, and the flatness of the surface is slightly better than that in BTA group. According to the density of the passive film, the rust inhibition effect is Na_2MoO_4 + BTA > BTA > Na_2MoO_4.

4. Conclusions

Under carbonation conditions, the main components of rebar passive film in cement paste mixed with rust inhibitor were FeOOH, Fe_3O_4, FeO, and Fe_2O_3. Among them,FeOOH and Fe_3O_4 played an excellent role in corrosion resistance.

Na_2MoO_4 reacted with Fe^{2+} to form $FeMoO_4$ protective layer, and BTA reacted with Fe to form N-Fe bonds.These two components improved the compactness of the passive film, thereby inhibiting rebar corrosion.

After adding of rust inhibitor, the composition and morphology of passive film are slightly different. According to the composition and compactness of the passive film, the effect of corrosion resistance is Na_2MoO_4 + BTA > BTA > Na_2MoO_4.

Acknowledgements

This work was sponsored by National Natural Science Foundation of China [No.52178223, No.51778302], Natural Science Foundation of Zhejiang Province [No. LQ20E080011].

REFERENCES

[1]J. Z. Liu, J. S. Shen, J. L. Yan, et al.Microstructure characteristics of steel corrosion products under carbonation and chloride corrosion,Journal of composite materials, 2018, **35**(09), 2587-2592.

[2] M. Liu,X. Q. Cheng,X. G. Li, et al. Effect of Cr on the passive film formation mechanism of steel rebarin saturatedcalcium hydroxide solution, Applied Surface Science,2016,389,1182-1191.

[3]Y. M. Cai, H. B. Zheng, X. Hu, et al. Comparative studies on passivation and corrosion behaviors of two types of steel bars in simulated concrete pore solution, Construction and Building Materials,2021,**266**(PA),120971.

[4] R. J. Mi,G. H. Pan,Q. Z. Shen. Carbonation modelling for cement-based materials considering influences of aggregate and interfacial transition zone, Construction and Building Materials,2019,229,116925.

[5] J. B. Wang,H. X. Xu,D. Y. Xu,et al. Accelerated carbonation of hardened cement pastes: Influence of porosity, Construction and Building Materials,2019,225,159-169.

[6]J. Liu, Q. W. Qiu, X. C. Chen, et al. Understanding the interacted mechanism between carbonation and chloride aerosol attack in ordinary Portland cement concrete, Cement and Concrete Research, 2017, 95, 217-225.

[7] J. Williamson, O.B.Isgor. The effect of simulated concrete pore solution composition and chlorides on the electronic properties of passive films on carbon steel rebar, Corrosion Science,2016,106, 82-95.

[8]J. Z. Liu, J. D. Geng, M. F. Ba, et al.Effect of nitrite on passivation film composition of reinforcing bar in the mortar containing chloride,Journal of building materials,2018,**21**(04), 536-541.

[9]J. G. Wei,X. H. Bian,W. Huang,et al.Passivation Behavior of Steel Bar in Sea Sand Ultra-high Performance Cement Evaluated Using Electrochemical Method,Acta silicate Sinica, 2020,**48**(08),1223-1232.

[10]H. Mohammed, B.Abdelillah, S.Latefa, et al. Chloride threshold value to initiate steel corrosion in simulated concrete pore solution, and the effectiveness of DMEA as an amino-alcohol-based corrosion inhibitor, Journal of Adhesion Science and Technology,2021,**35**(5), 504-521.

[11] M. Wu, J. J. Shi. Beneficial and detrimental impacts of molybdate on corrosion resistance of steels in alkaline concrete pore solution with high chloride contamination, Corrosion Science,2021,183,109326.

[12] Z. Y. Ai, W. Sun, J. Y. Jiang, et al.Passive behavior of new alloy corrosion resistant steel Cr10Mo1 in chloride-containing environment, Materials Guide,2016,**30**(15),92-99+118.

[13]Q. X. Li, Z. Y. Wang, W. Han, Characterization of the rust formed on weathering steel exposed to Qinghai salt lake atmosphere, Corrosion Science, 2008, **50**, 365.

[14]K. Arto, H. Mari, L. Jukka, Corrosion products of carbonation induced corrosion in existing reinforced concrete facades , Cement and Concrete Research, 2015, **78**, 200.

[15] Y. Zhou,Y.Zuo.Surface films on plasma nitrided stainless steel subjected to passivation treatments, Applied Surface Science,2015,353, 924-932.

[16]A.Alhozaimy,R. R. Hussain,A. Al-Negheimish, et al. Effect of Simulated Concrete Pore Solution Chemistry, Chloride Ions, and Temperature on Passive Layer Formed on Steel Reinforcement, ACI Materials Journal,2014,**111**(4),411-421.

[17] P.Ghods, O. B.Isgor, F.Bensebaa, et al. Angle-resolved XPS study of carbon steel passivity and chloride-induced depassivation in simulated concrete pore solution, Corrosion Science,2012,**58**,159-167.

[18]J. C. Zhang,J. Y. Jiang,Y. Li,et al.Passive Films Formed on Seawater Corrosion Resistant Rebar 00Cr10MoV in Simulated Concrete Pore Solutions,Journal of Chinese Society for Corrosion and Protection,2016,**36**(05),441-449.

[19] B. Lin, J. L. Tang, Y. Y. Wang, et al. Study on synergistic corrosion inhibition effect between calcium lignosulfonate (CLS) and inorganic inhibitors on Q235 carbon steel in alkaline environment with Cl^-, Molecules,2020,**25**(18),4200.

[20]B. H. Shang,Y. T. Mang,M. J. Meng,et al.Characterisation of Passive Film on HRB400 Steel Rebar in Curing Stage of Concrete,Journal of materials research,2019,**33**(09), 659-665.

****